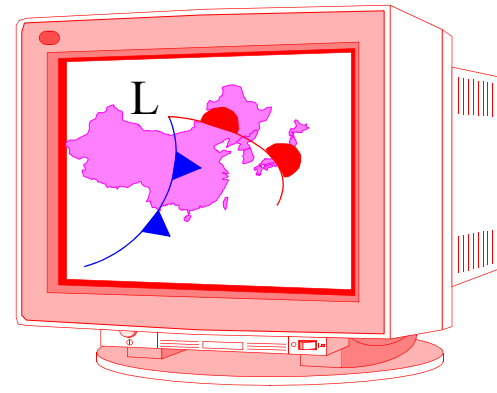
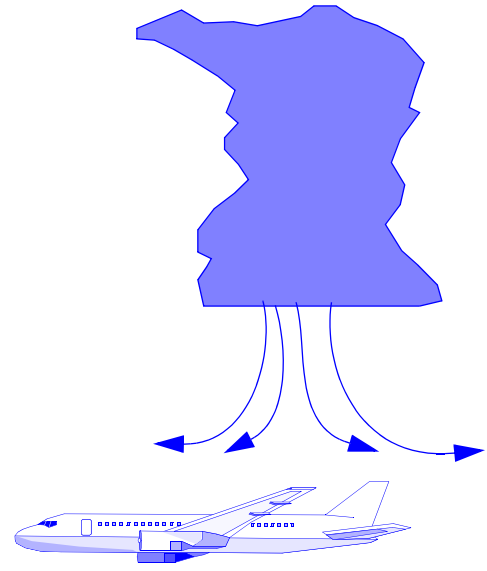


Bistatic Radar Networks

Forecasting Models

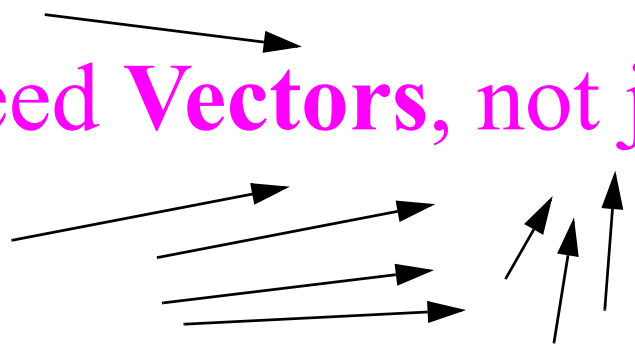


Airport Warning Systems



Scientists

need **Vectors**, not just Doppler radial winds



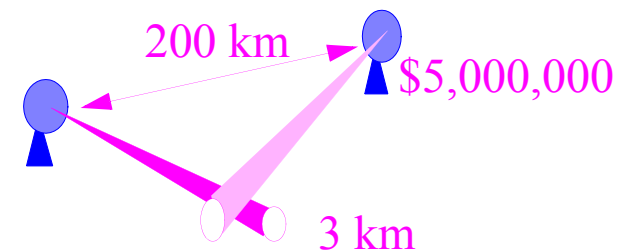
Vector winds can be measured or calculated

Multiple-Doppler Networks

Costly (WSR-88D's ~\$5,000,000 each)

Long baselines (~200 km in USA) = ~3 km resolution

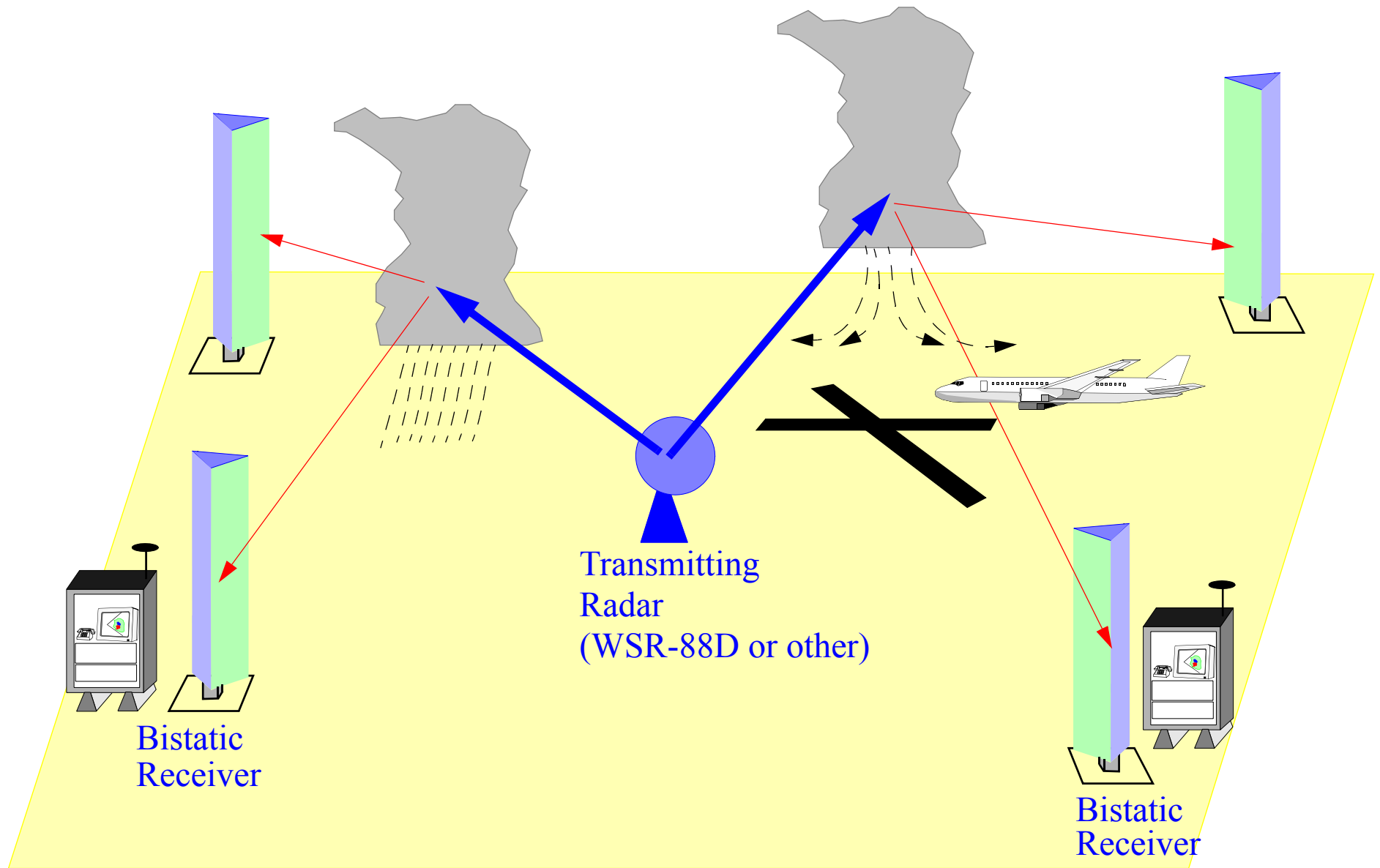
Long baselines = beams far from surface



Single-Doppler Retrievals

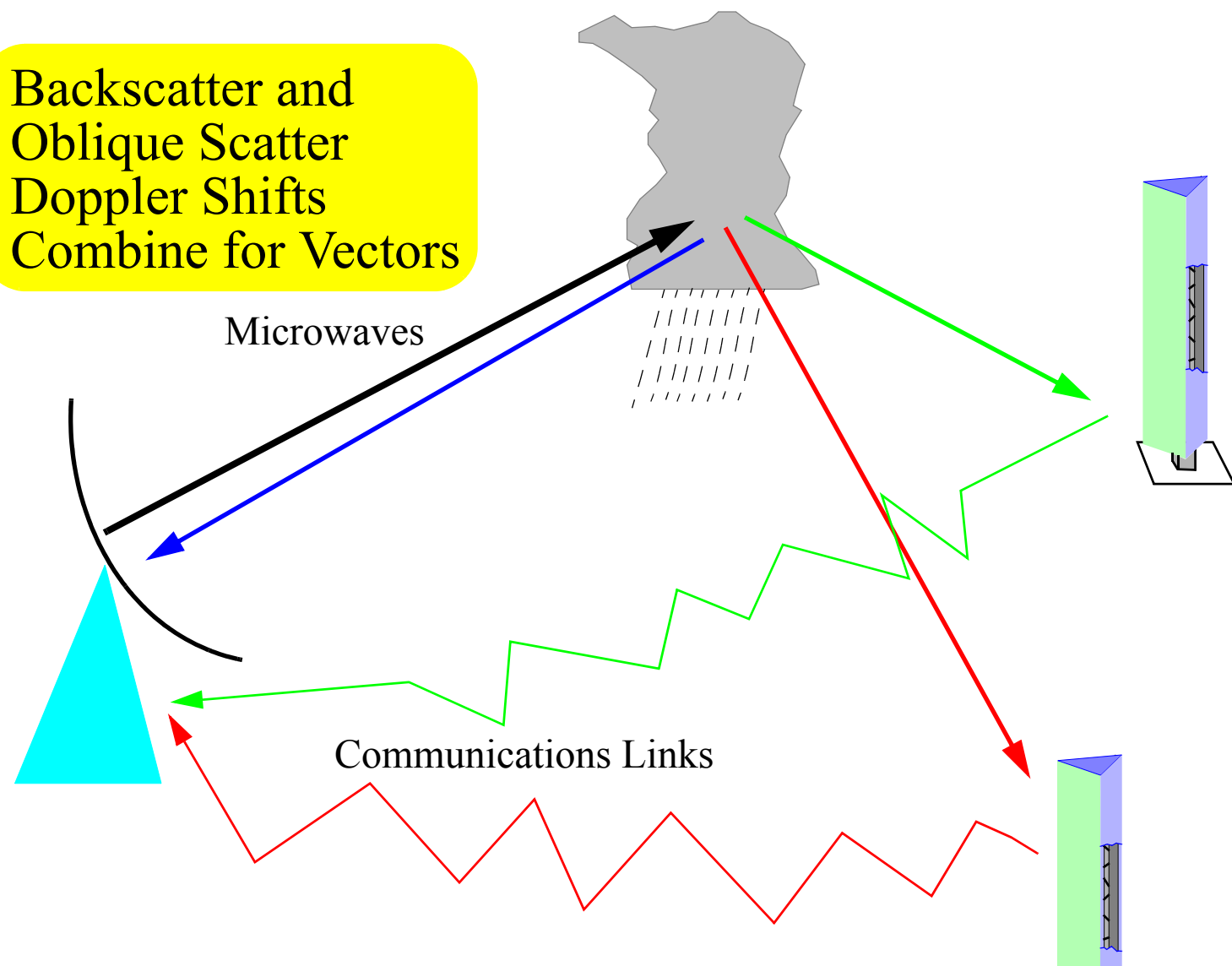
Not always possible, particularly in spotty convection

Prone to errors, sometimes in most interesting weather



Bistatic Radar Networks Provide Vector Winds

Backscatter and
Oblique Scatter
Doppler Shifts
Combine for Vectors



— Monostatic Doppler
— Bistatic Doppler #1
— Bistatic Doppler #2

} Vectors (u,v,w)

How Bistatic Networks Get Dual-Doppler Information

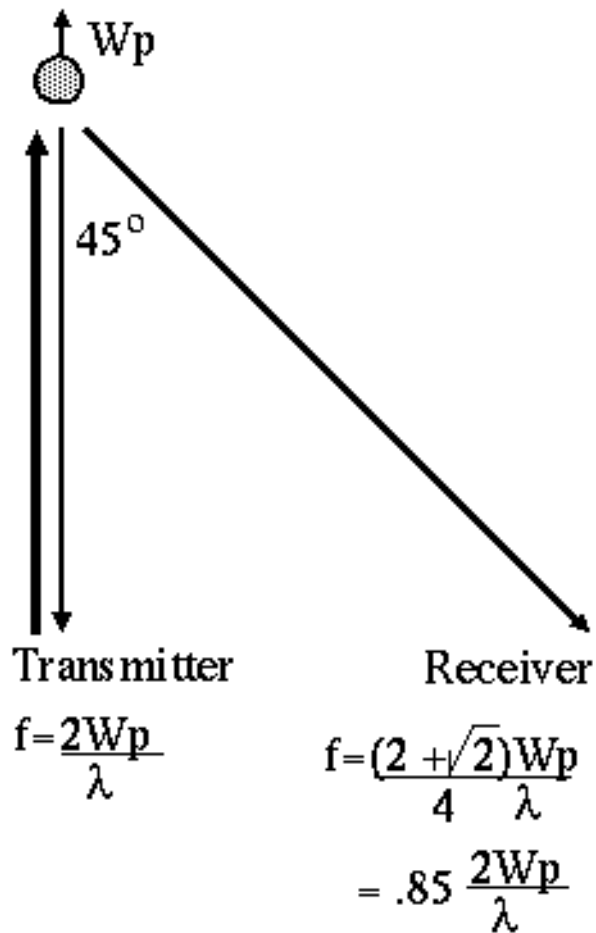


Fig. 5. Schematic diagram illustrating Doppler shifts measured at a monostatic transmitter/receiver and at a bistatic receiver after scattering from a particle exhibiting purely vertical motion.

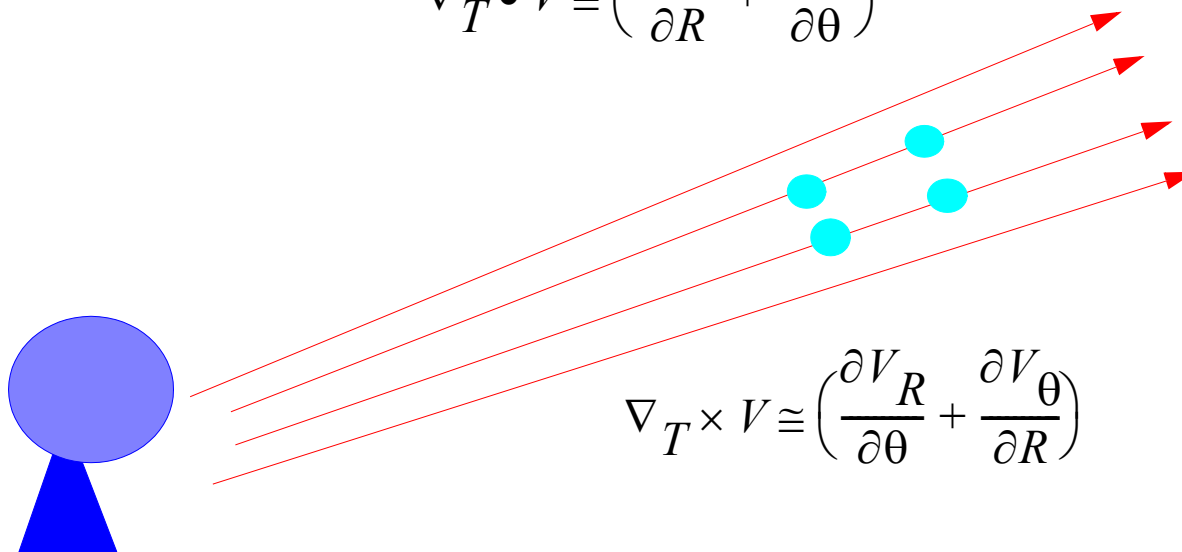
Advantages of Bistatic Multiple-Doppler Networks

1. **Cost:** Capital: <\$500,000 for basic network,
<\$100,000 for each additional receiver
(or less, depending on configuration)

Operations: no operators, no moving parts,
no high voltage, no large antennas.
< \$10,000 per receiver per year
2. **Simultaneous** measurements from only one source of illumination:
Reconstruction of u,v,w fields are from co-temporal data
and are true snapshots.
3. **No interpolation** or smoothing to Cartesian grids
4. Multiple-Doppler fields as fast as one radar can scan.
5. **Bistatic Network provides new Doppler processing and display for Tx**
6. Hail detection through polarization and bistatic LDR method (experimental)

Windshear (Divergence and Vorticity) is calculated at
high resolution in real-time
for *every* transmitted gate

$$\nabla_T \cdot V \cong \left(\frac{\partial V_R}{\partial R} + \frac{\partial V_\theta}{\partial \theta} \right)$$

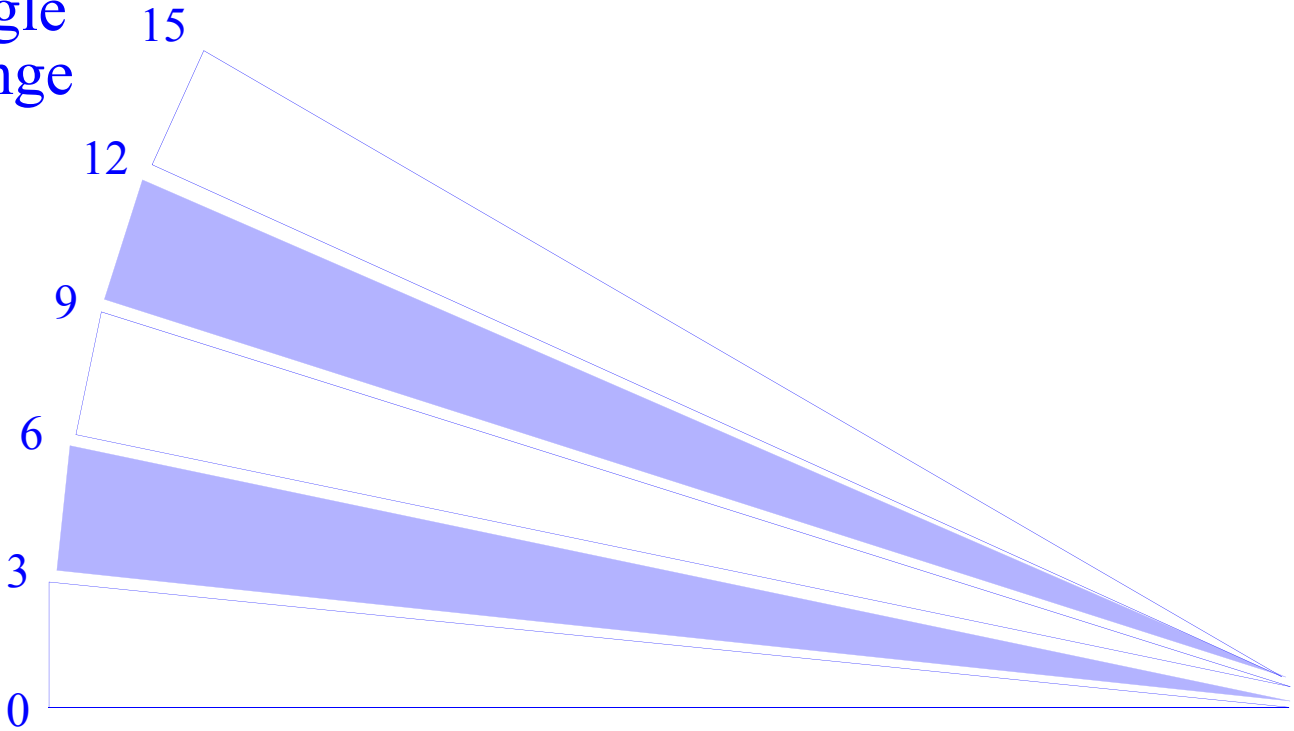


$$\nabla_T \times V \cong \left(\frac{\partial V_R}{\partial \theta} - \frac{\partial V_\theta}{\partial R} \right)$$

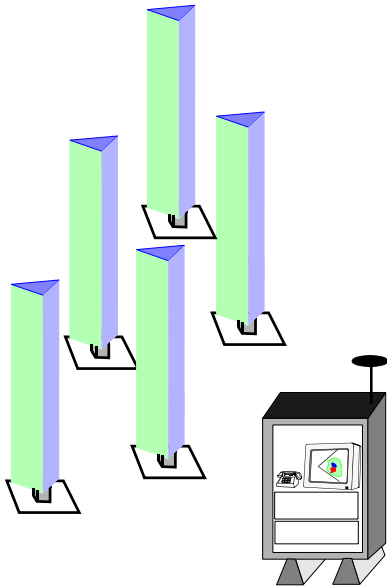
No Cartesian interpolation and smoothing necessary

Combination of several low cost higher gain antennas to improve sensitivity

Elevation
Angle
Range

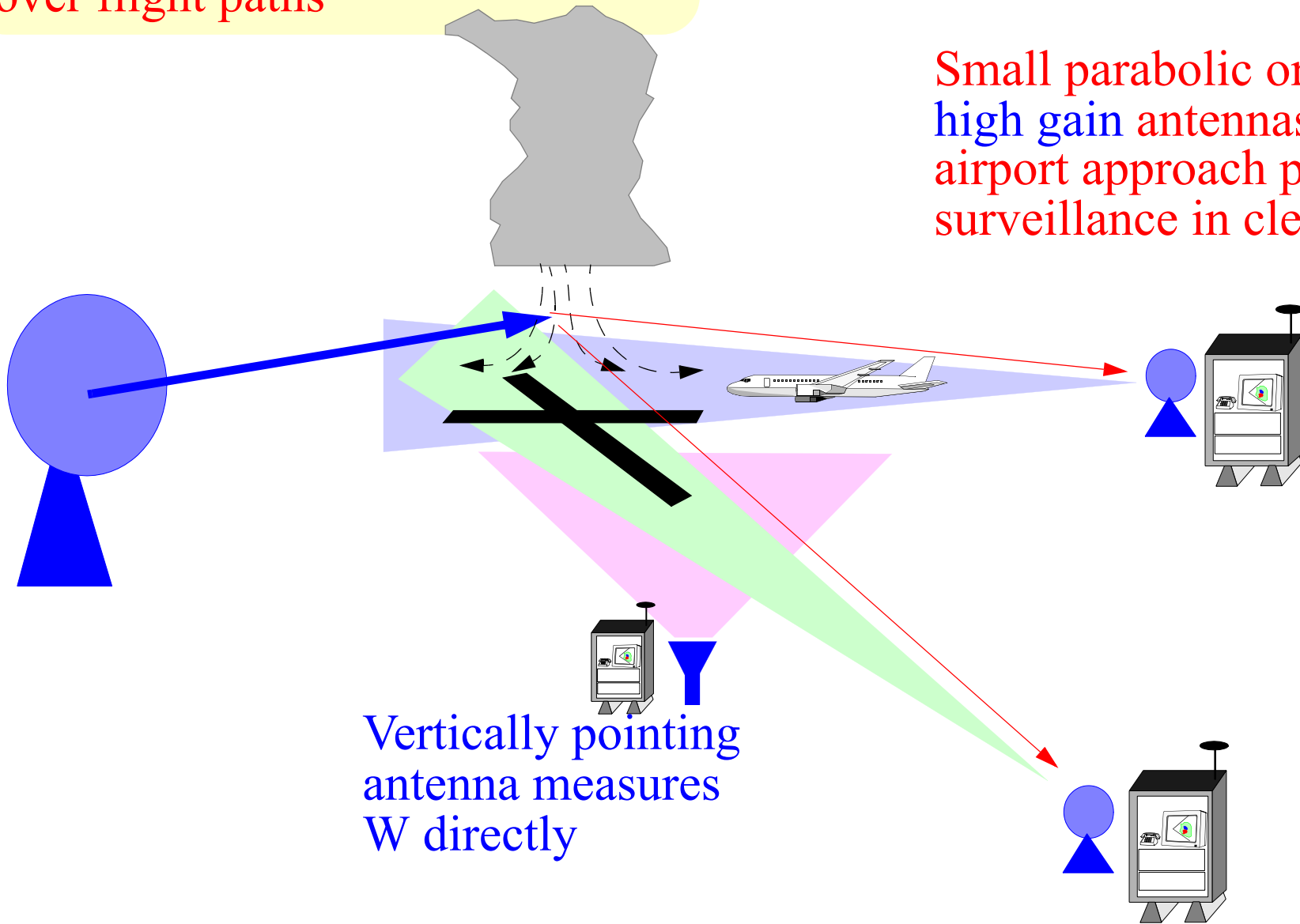


Electronic switching
as Tx antenna scans



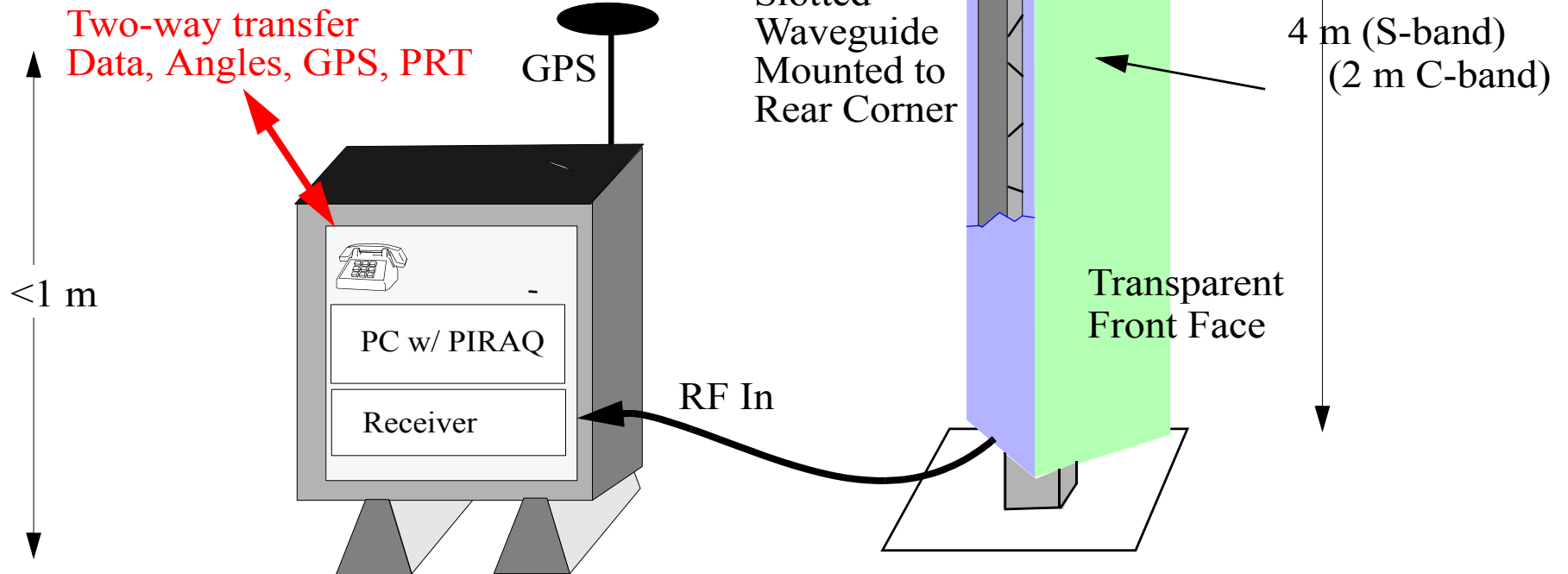
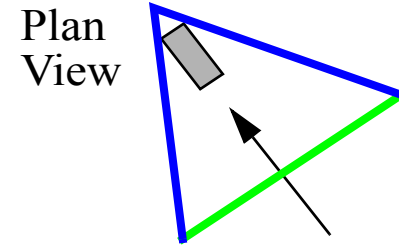
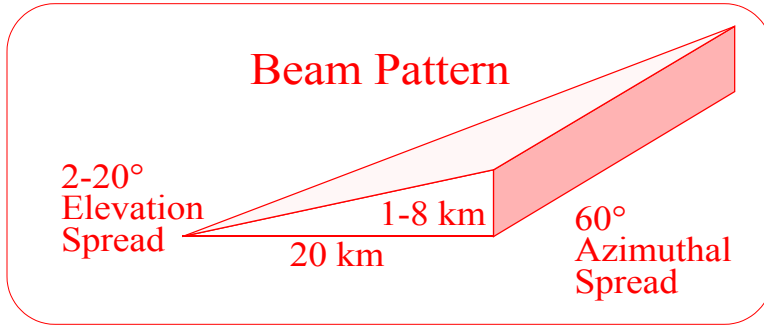
High Sensitivity Multiple-Doppler
Vector Winds and W
over flight paths

Small parabolic or other
high gain antennas for
airport approach path
surveillance in clear air



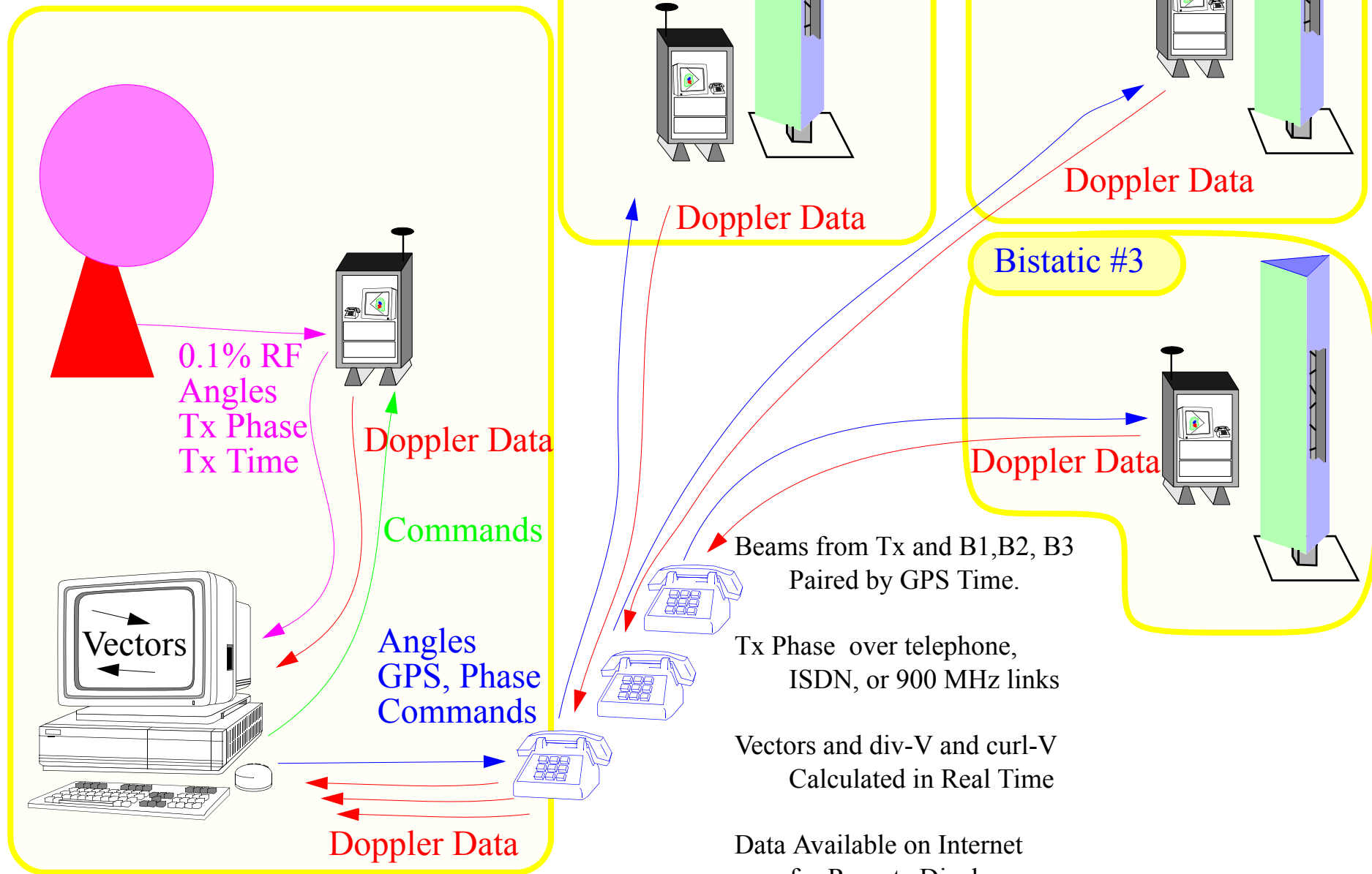
Vertically pointing
antenna measures
 W directly

Bistatic Receiver Sites

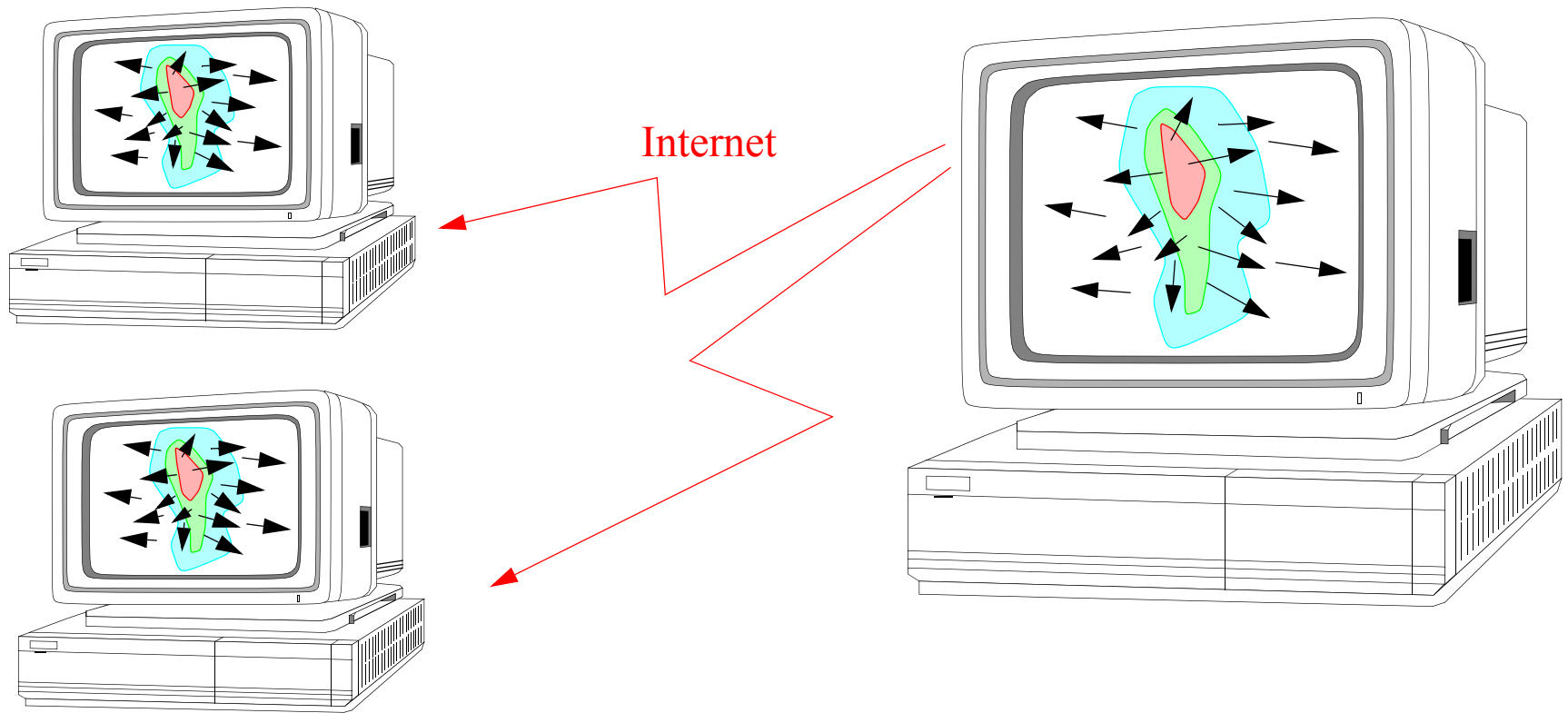


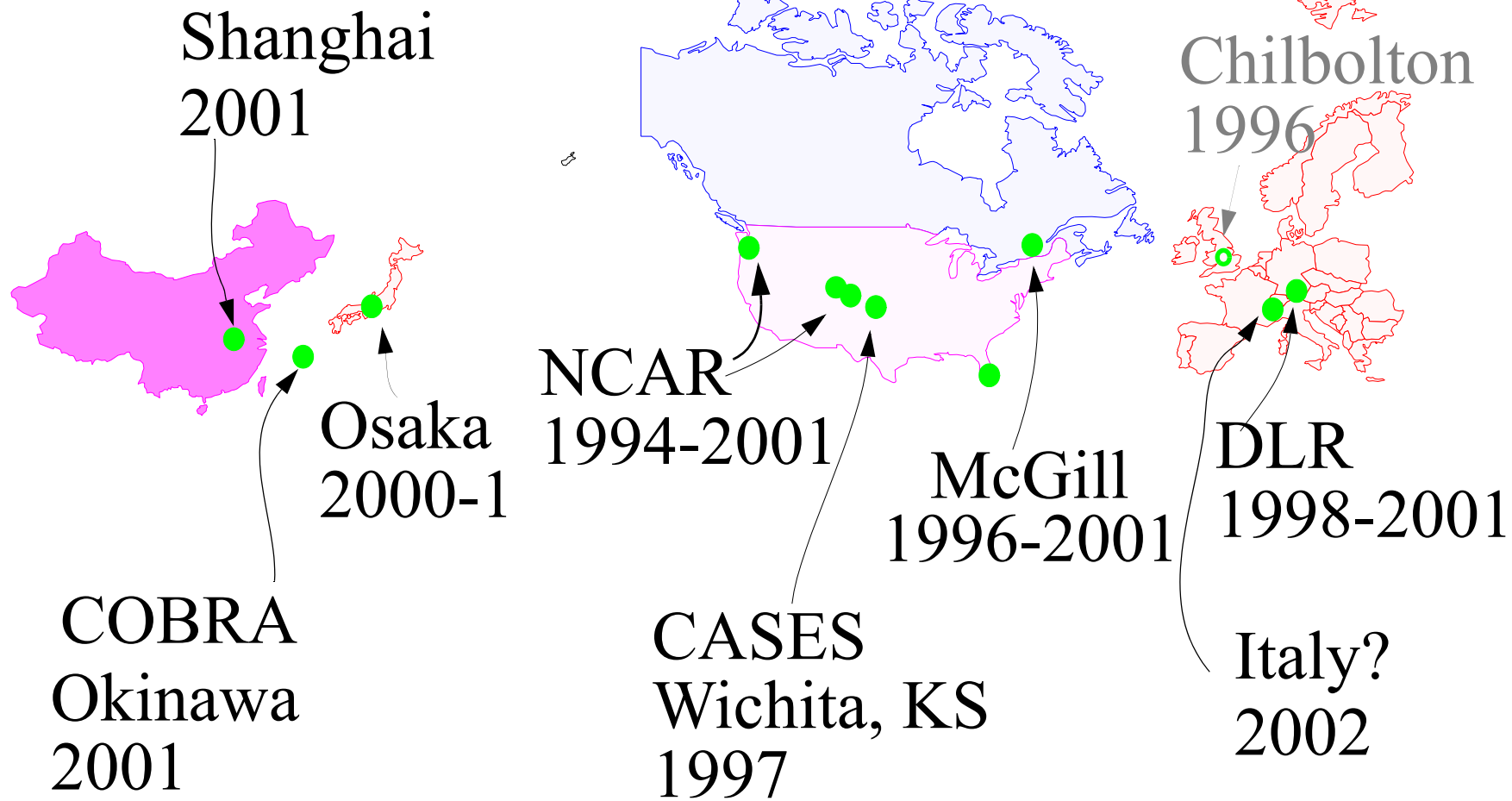
Current Bistatic Network Design

Klystron or Magnetron Transmitter
S, C, or X band



Real-Time Vector Displays Across Internet





Past, Present and Future
Bistatic Networks

Early NCAR Experiments

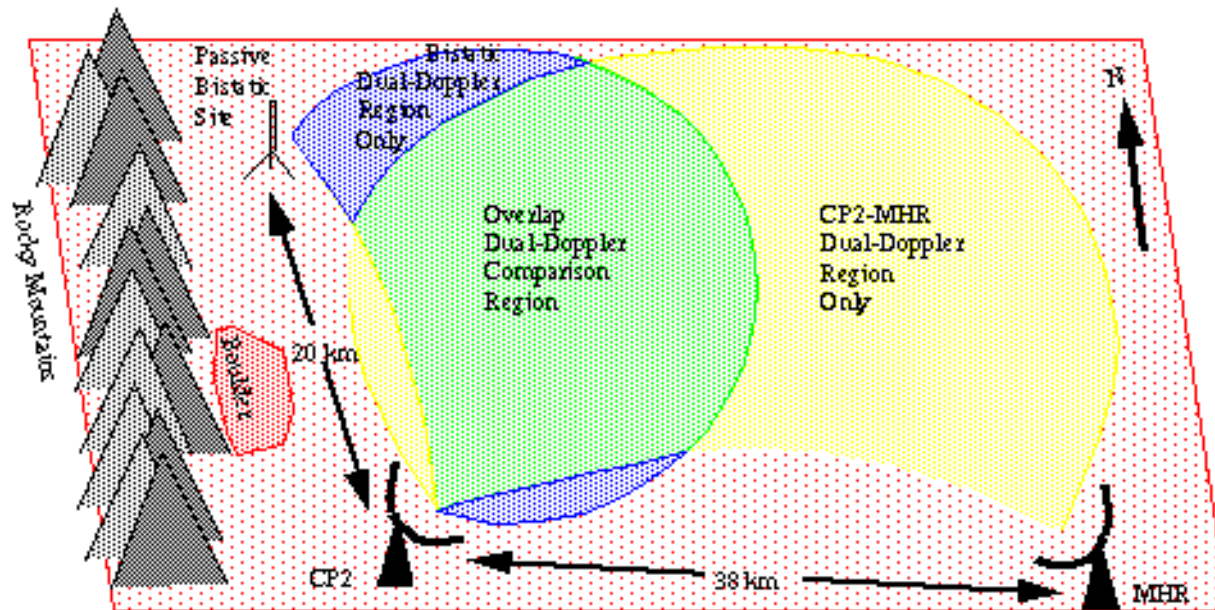
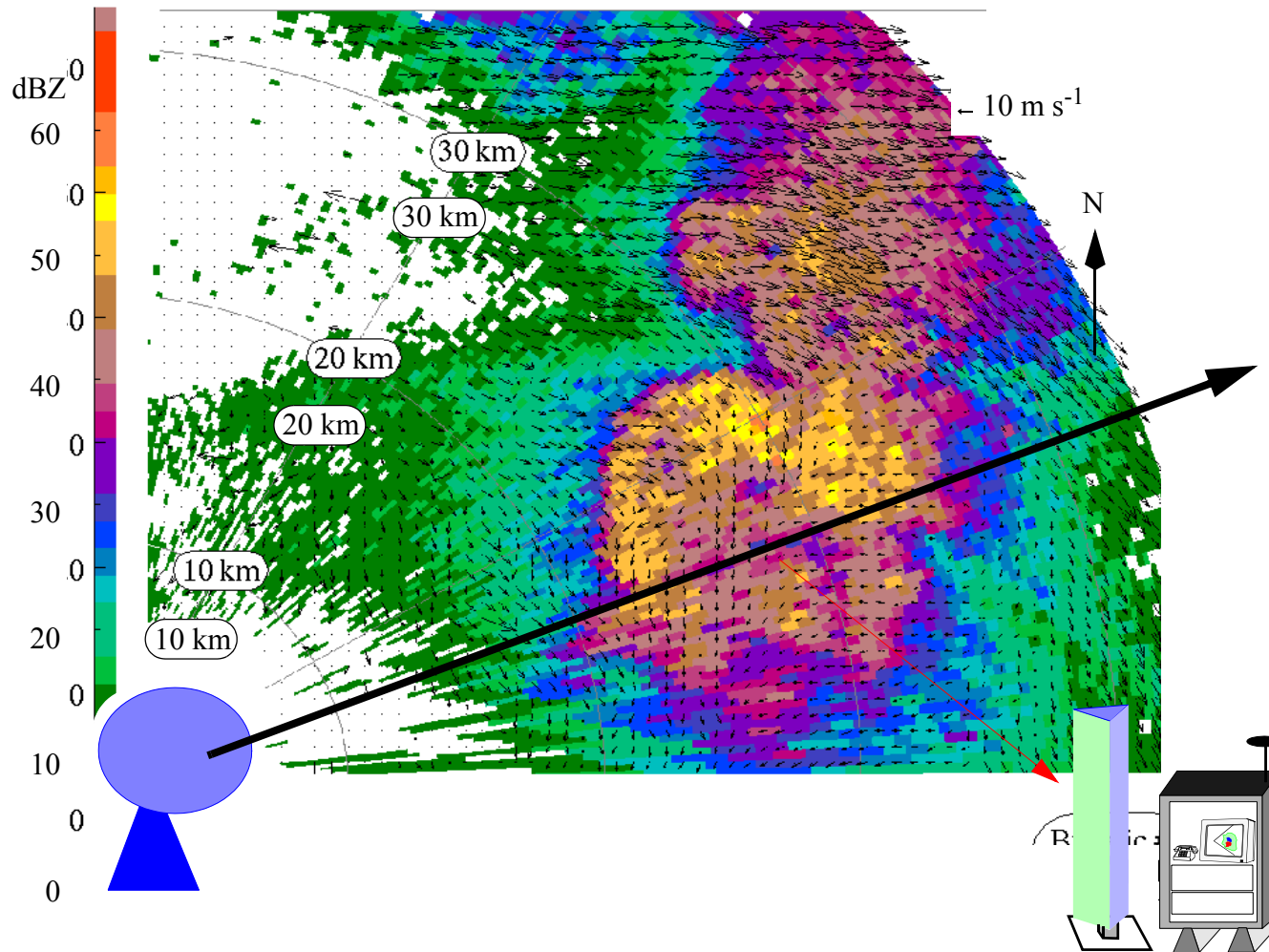


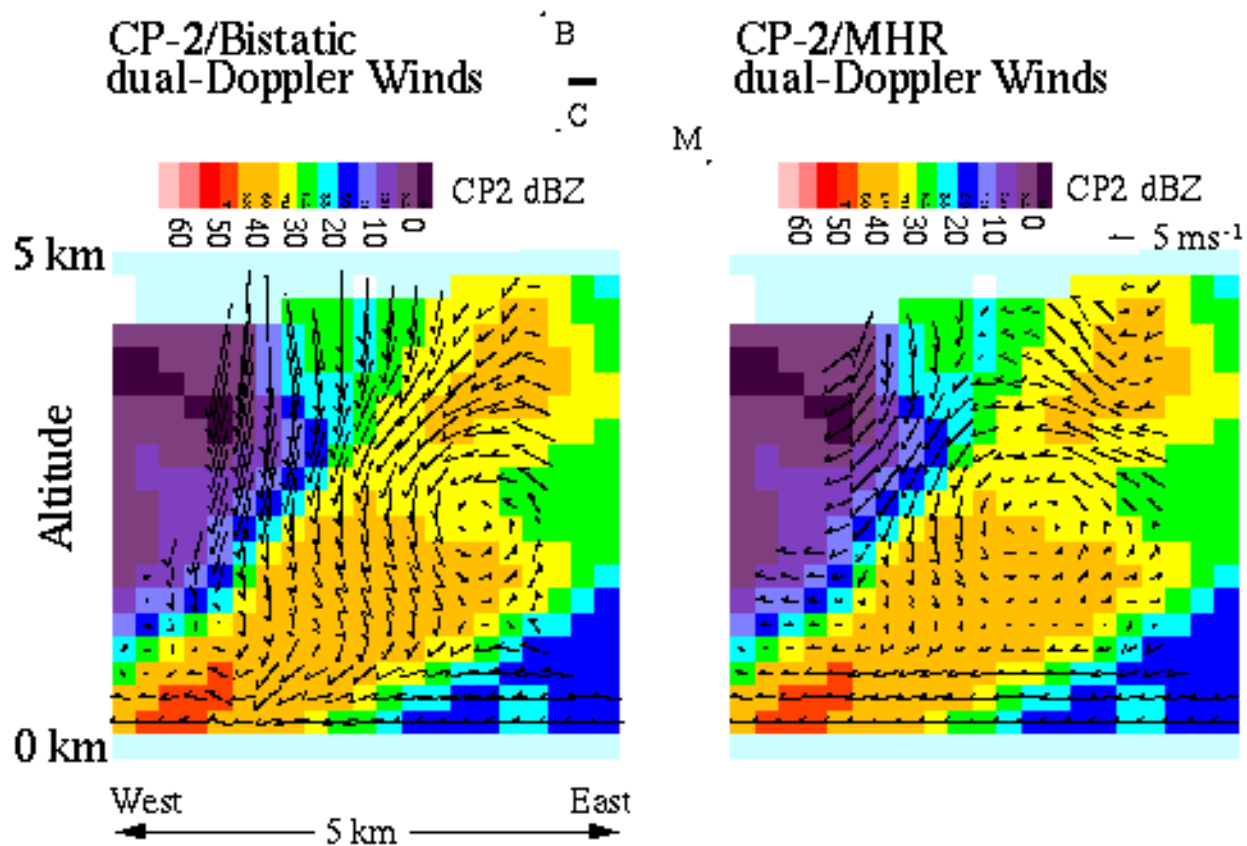
Figure 2: Deployment of radars during the 1993 prototyping experiment. The CP-2 transmitter was located south of Boulder, CO. The passive bistatic receiver was located 20 km to the north of CP-2, resulting in a dual-Doppler lobe extending to the east from Boulder. The MHR radar was located 38 km to the east of CP-2, resulting in a dual-Doppler lobe extending to the north. Comparisons of bistatic dual-Doppler vector winds (from CP-2 and bistatic data) and traditional monostatic dual-Doppler vector winds (from CP-2 and MHR data) were possible in the region in which the two lobes overlapped.

NCAR 1994-9:

Real Time Display of vector winds
as radar sweeps through weather



Reflectivity and Vector fields in thunderstorm



Validation

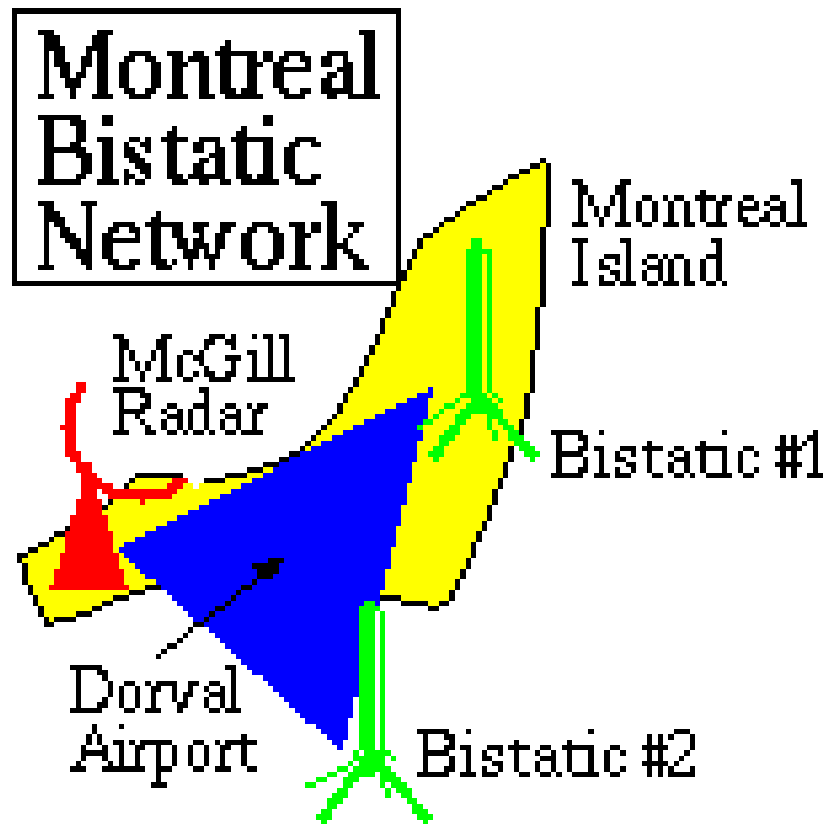
Figure 4: East-west vertical slice through weak convective cell. Vectors show slice parallel wind vectors calculated using CP-2 and bistatic data only (left) and CP-2 and MHR data only (right). Shading in both panels CP-2 measured reflectivity. Updraft is visible in both calculations at the eastern (rightmost) edge of the cell. Downdraft is visible in both calculations in the high reflectivity region of the cell. The downdraft is stronger in the CP-2/Bistatic retrieval. Inset labelled B,C,M with horizontal line indicates location of plot area relative to the three radar sites.



McGill (Montreal)
Receiver #1
(Isztar Zawadzki's house)
Equipment in House



NCAR (CASES-97)
Temporary Rx #2
Farmer's Field
Cage to Stop Animals



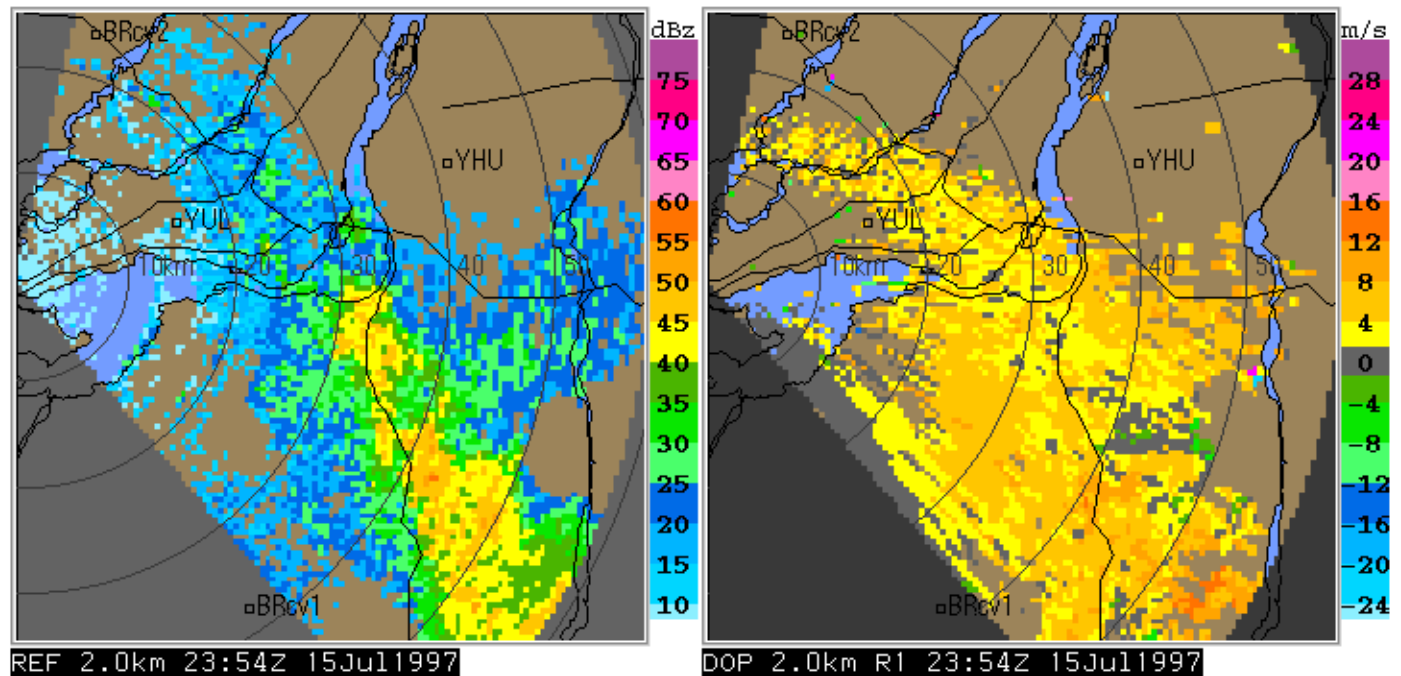
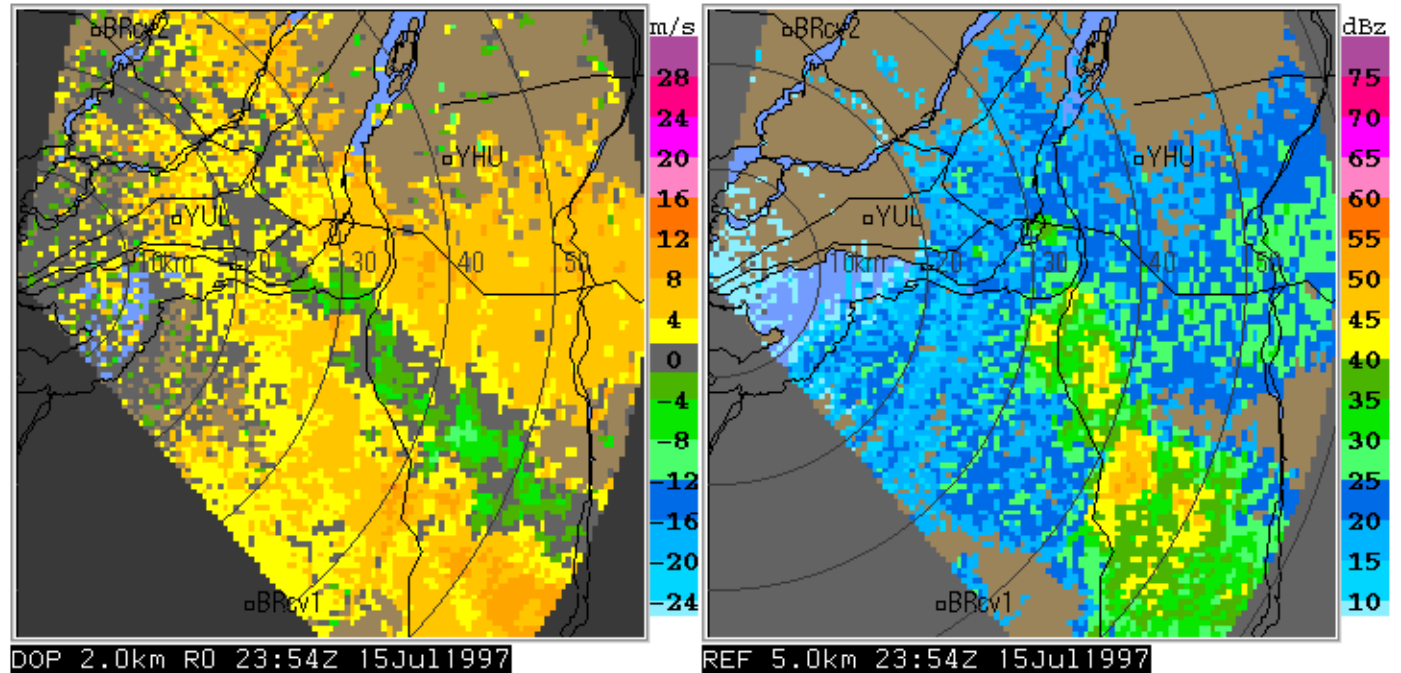
Baselines 40 km, 25 km

McGill 1996-9

Cartesian
Products

Variational
Techniques

Bouyancy
Temperature
Products

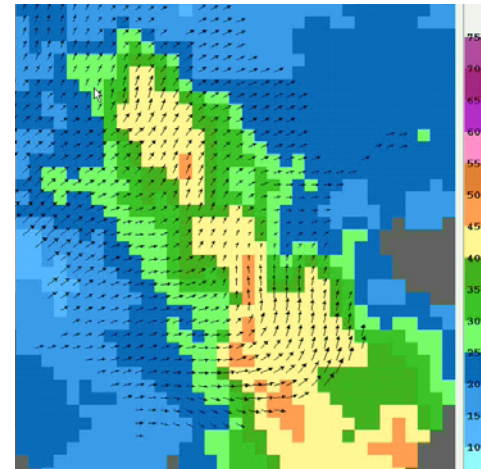


McGill Network

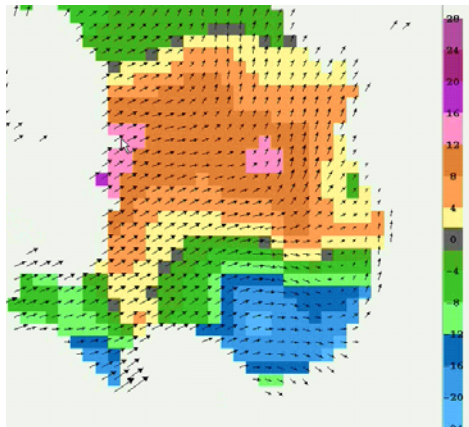
Cartesianized Data

T', P', W, $\nabla \times V$ retrievals

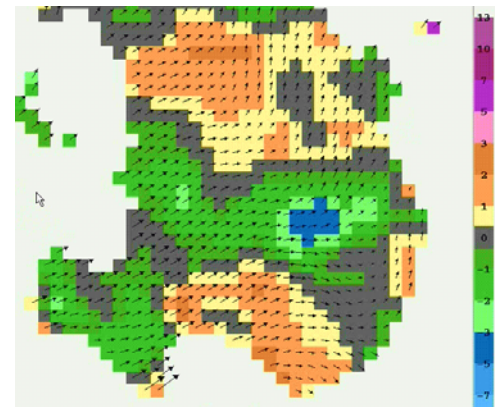
Vectors and dBZ



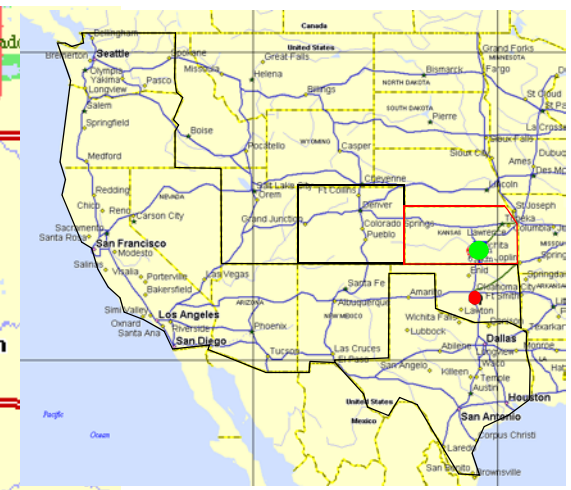
Vectors and T



Vectors and W



(Source: grappa.meteo.mcgill.ca/~protat)



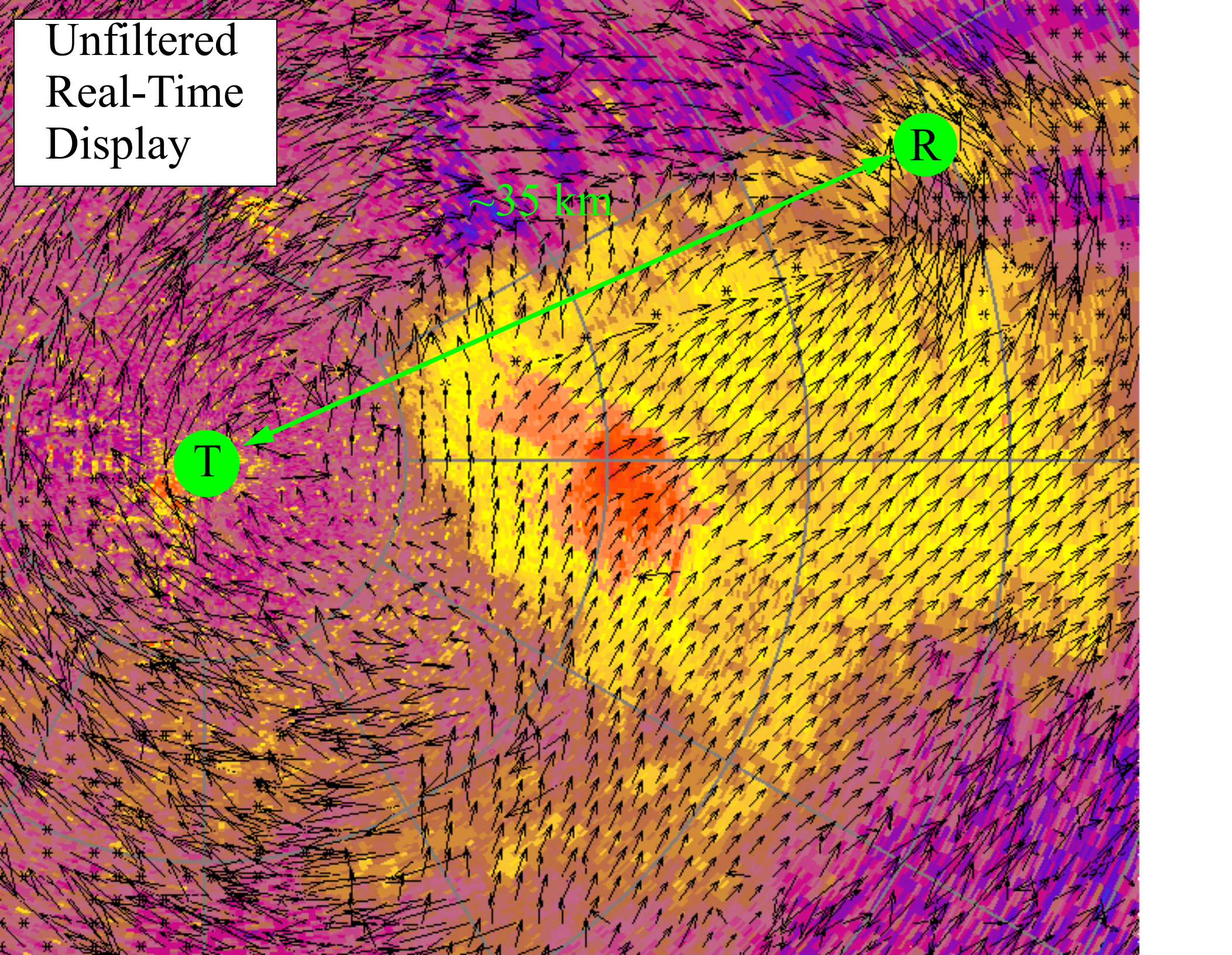
CASES
1997

NCAR

Wichita
Kansas

Temporary
Deployment
900 MHz
comm links

Unfiltered
Real-Time
Display



DLR: South of Munich, Germany

First Receiver Installed late 1998

Some test data in clear air only.

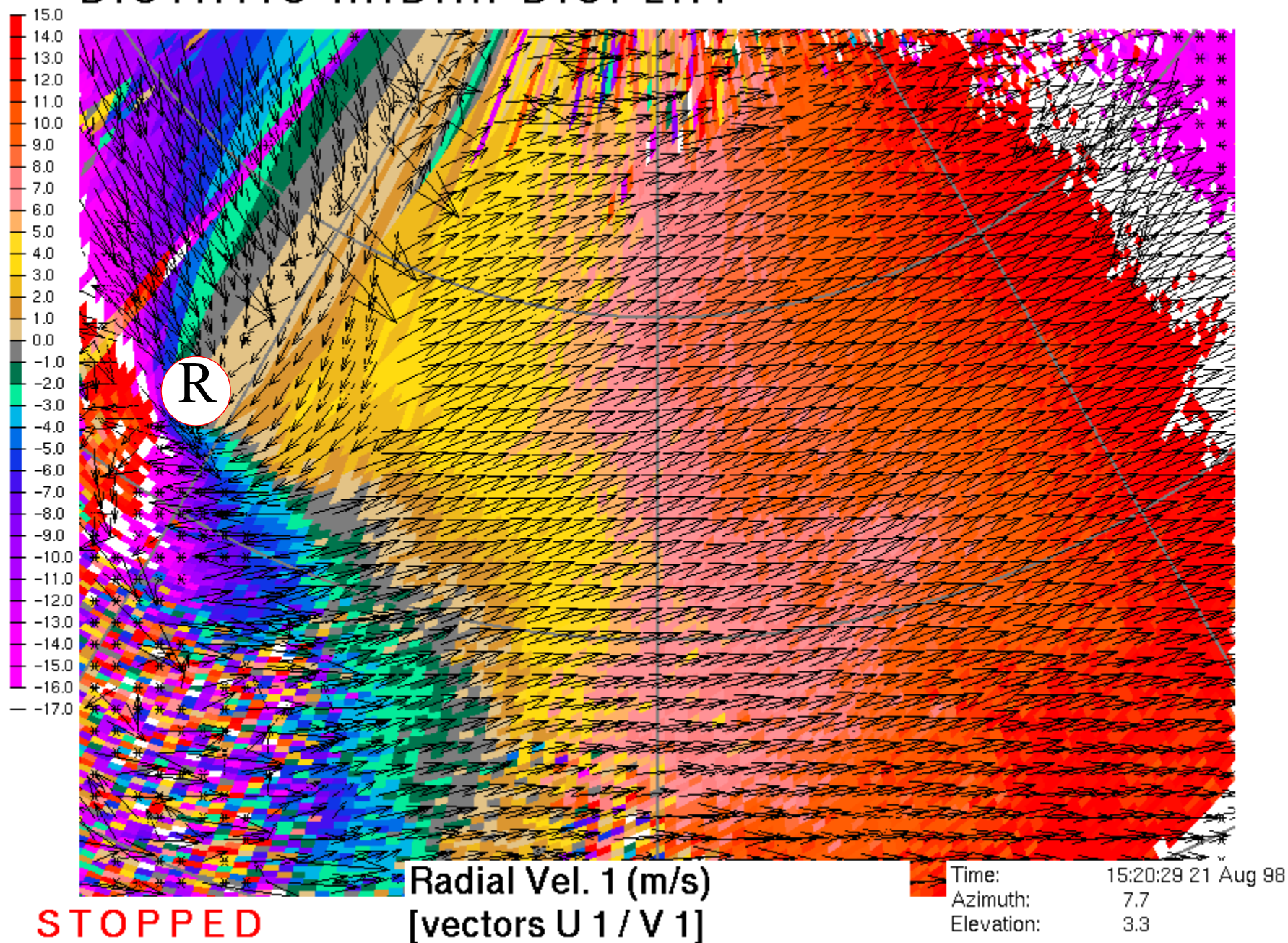
Second and Third Receivers Completed
in Fall 1999.

Baseline of 1st Receiver 27 km

Baselines of 2nd+3rd Receivers: 40-60 km

BISTATIC RADAR DISPLAY

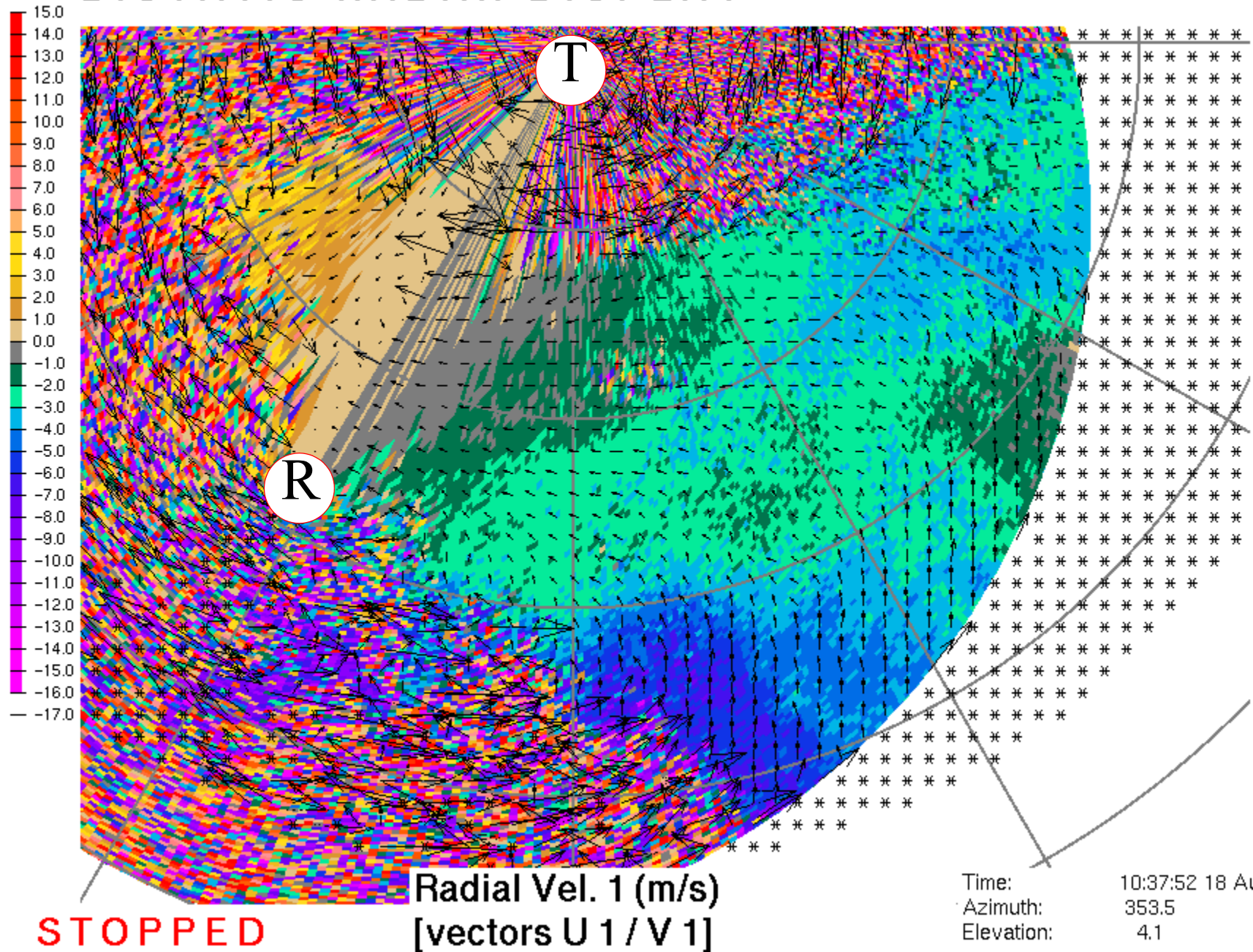
← 10.0 m/s



Raw Real-Time DLR Data: Wind vectors over Dopp Vel

BISTATIC RADAR DISPLAY

← 10.0 m/s



Raw Real-Time DLR Data: Wind vectors over Dopp Vel

Bistatic Networks

Year/Location	Wavelength	Tx Type	Comm Link
1993 Boulder	10 cm	klystron	direct line-of-sight
1994 Boulder	10 cm	klystron	telephone
1996 Chilbolton/Reading	10 cm	magnetron (pseudo-bistatic)	-----
1996-8 Montreal	10 cm	klystron	telephone
1997 Kansas	10 cm	klystron	900 MHz
1998-9 Munich Germany	5 cm	magnetron	ISDN
2000 Osaka	3 cm	magnetron	ISDN
1999 Oklahoma	3 cm	magnetron mobile DOW	900 MHz
2000 Washington	10 cm	klystron	900 MHz
2001 China	3 cm	magnetron	900 MHz
2001 Okinawa	5-10 cm	klystron	ISDN
2002 Italy	5	magnetron	unknown
2002 Korea	5	magnetron	unknown